



1 **Statistical and neural network assessment of climatological**
2 **features of fog and mist at Pula airport in Croatia: from local to**
3 **synoptic scale**

4

5 Marko Zoldoš^{*1,2}, Tomislav Džoić^{*3}, Jadran Jurković², Frano Matic⁴, Sandra Jambrošić², Ivan
6 Ljuština², Maja Telišman Prtenjak⁵

7

8 ¹Risk Management Division, Erste & Steiermärkische Bank d.d., Rijeka 51000, Croatia (ORCID: 0009-0005-1117-
9 5716)

10 ²Aviation Meteorology department, Croatia Control Ltd., Velika Gorica 10410, Croatia

11 ³Laboratory of Physical Oceanography, Institute of Oceanography and Fisheries, Split 21000, Croatia

12 ⁴Department of Marine Studies, University of Split, Split 21000, Croatia (ORCID: 0000-0003-0392-4172)

13 ⁵Department of Geophysics, Faculty of Science, University of Zagreb, Zagreb 10000, Croatia (ORCID: 0000-0002-
14 4941-8278)

15

16

17 **Leading author: Marko Zoldoš, correspondence to: Tomislav Džoić (dzoic@izor.hr)*

18

19

20 **Abstract.** A study was conducted on the climatological characteristics of fog and mist at Pula Airport in the
21 northeastern Adriatic, using statistical and machine learning approaches. The study utilized meteorological data from
22 Pula Airport, along with satellite sea surface temperature (SST) data from two coastal areas west and east of the
23 airport, to gain insights into the influence of sea temperature on fog formation. To identify weather patterns associated
24 with the occurrence of fog and mist, wind and mean sea-level pressure (MSLP) data from the ERA5 reanalysis were
25 analyzed using Growing Neural Gas (GNG), a machine learning method. A notable finding was a declining trend in
26 the frequency of fog and mist at the airport, which can be linked to the results of the GNG analysis of the ERA5 data.
27 This analysis showed a decrease in synoptic patterns favorable for fog and mist. Fog occurs mainly between October
28 and March and is primarily associated with weak easterly and northeasterly winds. Additionally, fog is more likely to
29 occur when the sea surface temperature is higher than the air temperature. Mist has similar characteristics to fog,
30 although it is more likely to occur with easterly winds.

31

32

33

34

35

36



37 1 Introduction

38 According to the World Meteorological Organization (WMO), fog is defined as the suspension of extremely tiny water
39 droplets or ice crystals in the atmosphere, often at a microscopic scale. This natural occurrence significantly reduces
40 visibility on the Earth's surface to less than 1 km (WMO, 1966). The formation of these minuscule water droplets and
41 ice crystals is influenced by various factors, including cooling, increased humidity, and the mixing of air masses with
42 different temperatures (Gultepe, 2007). Mist is a closely related phenomenon, occurring when horizontal visibility at
43 the surface is between 1 and 10 km. In aviation meteorology, mist specifically refers to conditions where surface
44 horizontal visibility is between 1 and 5 km. Fog is a unique atmospheric phenomenon confined to the atmospheric
45 boundary layer (ABL), the lowest part of the atmosphere, whose behavior and characteristics are directly influenced
46 by contact with the Earth's surface. The formation and dissipation of fog are profoundly impacted by synoptic and
47 mesoscale conditions, as well as surface features such as moisture sources (oceans, lakes, rivers), vegetation type,
48 orography, urban areas, and sea currents.

49

50 This study aims to investigate the occurrence of fog over an extended period at Pula Airport (44.89°N, 13.92°E),
51 located in the coastal region of Croatia in the northeastern Adriatic (Figure 1). The Adriatic Sea is a large semi-
52 enclosed sea separating the Apennine Peninsula from the Balkans. It is the northernmost arm of the Mediterranean
53 Sea, extending from the Strait of Otranto (where it connects to the Ionian Sea and the rest of the Mediterranean) to the
54 northwest, toward the Po Valley and the Istria Peninsula. This region is prone to marine fog formation due to synoptic-
55 scale effects that can trigger subsidence within the boundary layer, causing stratus clouds to descend to the surface.
56 Similar marine fog events have been observed and analyzed in other regions like the northwestern Pacific and Atlantic
57 Oceans (e.g., Koračin et al., 2001; Koračin and Dorman, 2017). In the Adriatic region, fog is commonly observed
58 between September and May, often disrupting sea transport and port operations (Popović et al., 2014). In addition to
59 affecting sea traffic, fog is a major disruptor of air traffic because of safety, as fog at airports can cause significant
60 flight delays due to poor visibility and low cloud ceilings. These delays result in substantial financial losses for airlines,
61 underscoring the need for accurate fog forecasting. For example, dense fog at New Delhi Airport in India caused losses
62 of approximately 3.9 million U.S. dollars between 2011 and 2016 (Kulkarni et al., 2019). The importance of mitigating
63 these losses is highlighted by a study by Allan (2001), which estimated that improved forecasts during low ceiling/poor
64 visibility events at 3 airports in the New York City area could save up to \$240,000 per event.

65

66 These factors collectively emphasize the importance of fog research in improving the forecasting process.
67 Unfortunately, the study of fog remains an area of atmospheric science where our understanding is limited, both over
68 land (Gultepe, 2007) and ocean (Koračin and Dorman, 2017). Fog formation requires a fine interplay of processes
69 ranging from synoptic to microscale levels. The typical size of fog condensation nuclei is around $0.1 \mu\text{m}$ (10^{-5} cm),
70 while the synoptic-scale processes that contribute to fog development occur on a scale of 10^8 cm or more, making the
71 ratio of interacting length scales about 10^{13} . The full explanation of fog formation involves various elements, including
72 synoptic conditions (Belo-Pereira and Santos, 2016), land surface characteristics and radiation exchange (Duynderke,
73 1991), microphysics (Gultepe and Milbrandt, 2007; Wang et al., 2019), climatology (Stolaki et al., 2009; Veljović et



74 al., 2015; Belo-Pereira and Santos, 2016), relationships to turbulence intensity (Ju et al., 2020), aerosol (Oztaner and
75 Yilmaz, 2013), and more. Weather forecasting, the most publicly visible area of meteorology, involves not just
76 atmospheric science and its applications, but also communication and interaction with users. The forecasting process
77 always begins with the output from a numerical weather prediction (NWP) model, which, despite continual
78 development and upgrades, is not perfect and can only offer guidance (Tudor, 2010; Klaić, 2015; Telišman Prtenjak
79 et al., 2018). An expert forecaster must therefore use both general knowledge of large-scale weather systems and
80 detailed knowledge of local processes and climatology to refine this guidance into a final forecast product. The
81 complicated interplay of meteorological parameters that leads to fog or no-fog conditions makes fog forecasting a
82 significant challenge (Bergot and Koraćin, 2021).

83

84 This investigation focuses on analyzing the climatological characteristics of fog at Pula Airport (Croatia) and
85 understanding the general patterns of fog initiation and dissipation. The first goal is to provide detailed statistical
86 analyses to help understand the local and dynamic processes that lead to fog development. Another important goal is
87 to gain insight into the influence of sea surface temperature (SST) in the vicinity of the study area on the frequency
88 and intensity of advective fog, as SST has been shown to have a significant impact on the accuracy of NWP models
89 (Huang et al., 2022). For this study, an unsupervised machine learning algorithm called the Growing Neural Gas
90 Network (GNG), a method within artificial neural networks (Martinetz and Schulten, 1991), has been used. The main
91 aim of applying this method is to classify the synoptic conditions that prevail before and during the occurrence of fog
92 at Pula into different weather patterns, and to determine if there are patterns that favor fog development. The results
93 of this research could significantly help local forecasters improve fog forecasting by considering the specific terrain
94 and coastline features, as well as synoptic and local influences (particularly SST), thereby filling a gap in scientific
95 knowledge about fog characteristics in this part of the Mediterranean.

96 **2 Location, data and methods**

97 **2.1 Location**

98 Pula Airport is the international airport serving the coastal city of Pula (population 52,411, according to the 2021
99 census) in western Croatia. It is located approximately 6 km ENE of the city center (Figure 1b). The exact geographical
100 coordinates of the airport are 44°53'37" N and 13°55'20" E, with an elevation of 84 meters above mean sea level
101 (AMSL). In 2023, Pula Airport served 413,439 passengers, making it the fifth busiest airport in Croatia by passenger
102 traffic (source: <https://podaci.dzs.hr/2023/en/58556>). The airport is situated at the southern tip of the Istrian
103 Peninsula—the largest peninsula in the Adriatic Sea—positioned between the Gulf of Trieste to the northwest and the
104 Kvarner Gulf to the east. The climate of Istria is influenced by both the Alpine and Dinaric Alps mountain ranges, as
105 well as the Mediterranean Sea. Winters in Istria are typically mild and wet, while summers are hot and humid. The
106 interior of Istria experiences a more continental climate, while the coastal area is significantly influenced by the
107 Adriatic Sea. Recent research has analyzed bioclimatic parameters, highlighting these climatic boundaries across the
108 peninsula (e.g., Omazić et al., 2020).



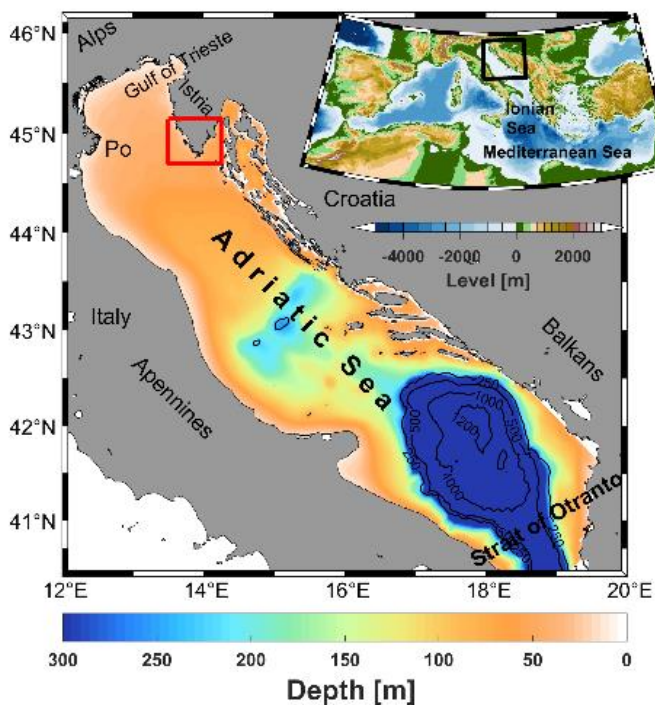
109

110 Two weather patterns are most commonly associated with fog in Pula. The first involves a predominantly westerly
111 flow that advects moist air from the west (W) and northwest (NW) under anticyclonic conditions. In these situations,
112 advection can occur over a wide geographical area. Fog is often advected from the Po Valley in northern Italy, where
113 it is a frequent phenomenon during the fall-winter season (Mariani, 2009), across the northern Adriatic to the shores
114 of Istria. In such weather patterns, fog can sometimes persist for days over the entire affected region (Bendix, 1994).
115 This is reflected in the fact that Linate Airport in Milan, Italy, was once the European airport with the most annual
116 shutdowns due to fog (Mariani, 2009). Although advective fog is not as common in the northwestern Adriatic, it still
117 occurs frequently on the western coast of Istria (Tešić and Brozinčević, 1974), which is climatologically the foggier
118 area of the eastern Adriatic (Stipaničić, 1972). The second weather pattern associated with fog in Pula involves a
119 predominantly easterly flow with advection from the southeast (SE) during a weakening anticyclone. These patterns
120 are closely related to broader atmospheric circulation over the Adriatic Sea, which is dominated by four main wind
121 field patterns. It is important to emphasize the influence of the wind regime, which includes the northeasterly (NE)
122 wind called bora and the southeasterly (SE) wind called sirocco, both typically occurring in the colder part of the year
123 and influenced by regional synoptic-scale systems. During the warmer part of the year, sea/land breezes and, to a
124 lesser extent, the Etesian wind are frequent. The change in wind at Pula Airport is influenced by these fundamental
125 wind regimes (e.g., Pandžić and Likso, 2005; Prtenjak and Grisogono, 2007; Prtenjak et al., 2010; Belušić et al., 2018).
126

127 The terrain surrounding the airport is mostly flat, covered with grass vegetation and small forests. In the immediate
128 vicinity, there are no notable hills or mountains that could significantly influence the weather and climate of the area.
129 The central part of the airport, along with the nearby southern surroundings, lies in a very shallow basin, which is
130 prone to nighttime inversions during calm wind conditions and clear skies (as reported by local forecasters). The sea
131 is very close to the airport—Pula Bay is just 6 km to the west-southwest, and the open waters of the northern Adriatic
132 Sea are 10 km away. To the east, the open sea is 7 km away, with the small Bay of Kavran situated just 5 km from
133 Pula Airport. These factors make the weather at the airport very susceptible to marine influence, even though the
134 airport itself is not directly on the coast.

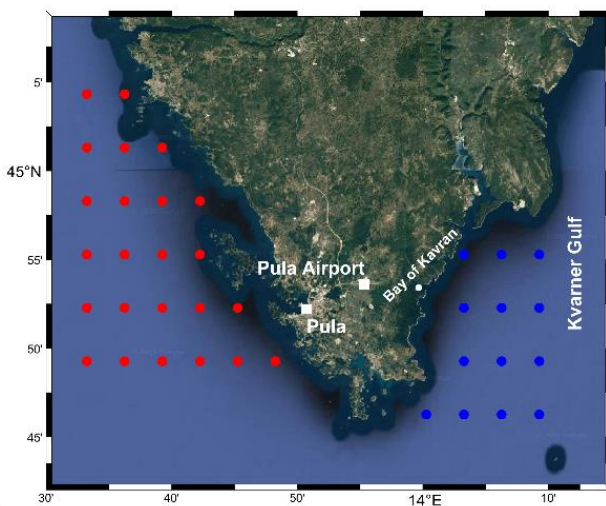
135

136



137

a)



138

b)

139 Figure 1. a) Map of the bathymetry of the Adriatic Sea, with the black square marking the area of the Adriatic Sea. The
140 red rectangle on the map marks the immediate surroundings of Pula Airport (b) (© Google Maps 20). The important
141 localities are marked with white squares, while blue and red dots mark the eastern and western grid points from which the
142 satellite SST values were extracted. The wider area of the Mediterranean Sea corresponds to the area of the ERA5
143 reanalysis. 24

144



145 **2.2 Data and methods**

146 The dataset used for this study includes half-hourly METAR reports and three-hourly SYNOP reports from the
147 meteorological station at Pula Airport. The meteorological variables considered are wind speed and direction,
148 temperature at 2 meters above ground, dew point temperature, relative humidity, surface pressure, cloud cover, and
149 horizontal visibility. These variables are reported by both station observers and automatic instruments. The dataset
150 spans a 20-year period from January 1, 2001, to December 31, 2020. All measurements were taken by instruments
151 located at the airport's meteorological station. Runway 27, the primary runway in use, is equipped with a landing
152 system capable of Category I operations. This allows for takeoff and landing under low visibility conditions with a
153 Runway Visual Range (RVR) of up to 550 meters or a ceiling height of 200 feet (approximately 60 meters). This
154 capability highlights the significant impact of fog on airport operations in Pula—when visibility drops below 550
155 meters, aircraft landings and takeoffs are not possible.

156

157 In addition to data from Pula Airport, daily sea surface temperature (SST) values from the Pula Bay oceanographic
158 station were utilized. This dataset includes SST measurements taken at 07:00, 14:00, and 21:00 local time from
159 January 1, 2001, to December 31, 2020. For the same period, reprocessed satellite data of SST in the Mediterranean
160 region were obtained from the Copernicus Marine Data Store (<https://data.marine.copernicus.eu/>). This dataset, which
161 has been optimally interpolated (level 4) with a grid resolution of 0.05° (Merchant et al., 2019), provides a
162 comprehensive view of sea surface temperatures. Two coastal areas were selected for analysis: one to the west of the
163 airport towards the open Adriatic Sea and the other to the east towards the Kvarner Gulf (Figure 1). The purpose of
164 this selection was to extract the average spatial SST for these two regions on a given day and assess their influence on
165 fog formation. These areas were chosen because they encompass the nearshore sea where the most frequent winds
166 occur.

167

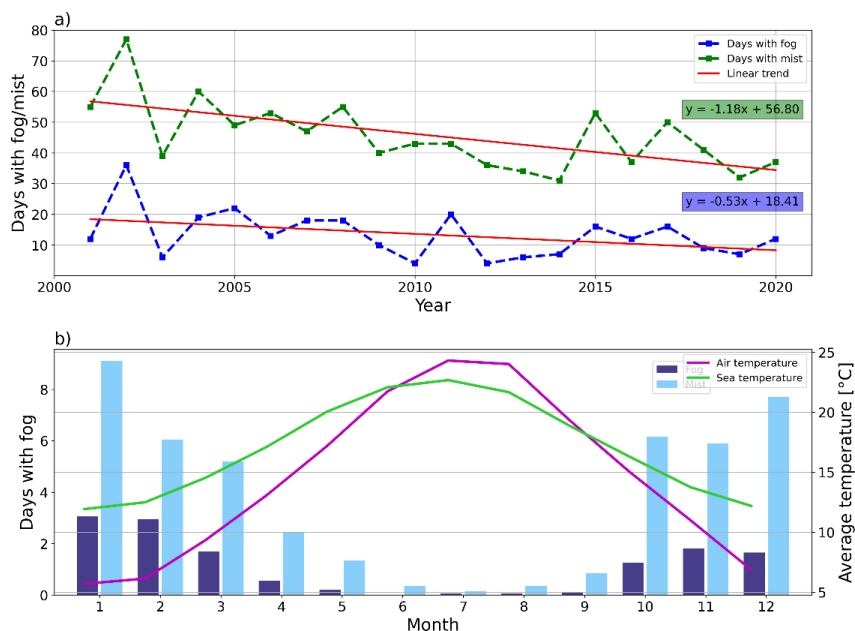
168 To identify the synoptic wind and pressure fields that favored fog occurrence at Pula Airport and across the
169 Mediterranean region, 10-meter wind and mean sea-level pressure (MSLP) data were sourced from the fifth generation
170 of ECMWF's ERA5 reanalysis. This reanalysis provides a comprehensive view of global climate and weather from
171 the last 4 to 7 decades. ERA5 integrates observational data with atmospheric models to deliver detailed and accurate
172 assessments of past weather. It has a horizontal resolution of 0.25° for latitude and longitude, a temporal resolution of
173 one hour, and a vertical resolution based on 37 pressure levels (Hersbach et al., 2020a; 2020b). The covered area
174 extends from 20°W to 40°E and 25°N to 55°N (Figure 1a, smaller map), with data spanning from 1979 to 2019. To
175 manage the large datasets of 10-meter wind and MSLP and classify them into spatio-temporal patterns that shed light
176 on atmospheric conditions favoring fog formation at Pula Airport, the Growing Neural Gas Network (GNG) method
177 was employed. GNG is an unsupervised artificial neural network that clusters high-dimensional input data by reducing
178 its dimensions and grouping it into best matching units (BMUs) (Fritzke, 1995). Unlike traditional neural networks
179 with fixed structures, GNG dynamically expands by adding new neurons in response to input patterns. This ability to
180 grow and adapt allows GNG to effectively cluster data and detect patterns and anomalies. The GNG algorithm has
181 been successfully used to detect anomalies in Adriatic Sea data, combining various biological and oceanographic



182 inputs (Šantić et al., 2021; Džoić et al., 2022). In this study, the method outlined in Matić et al. (2022) was applied to
183 a high-dimensional, 40-year dataset with wind components u and v for the entire year. Nine BMUs per month were
184 calculated for each month of the year using the GNG algorithm from the Python library NeuPy. Data processing and
185 visualization were performed using Python and MATLAB, with MATLAB employing the mapping package M_map
186 (Pawłowicz, 2020) which is available online at www.eoas.ubc.ca/~rich/map.html.

187 3 Results and discussion

188 3.1 Climatological analysis

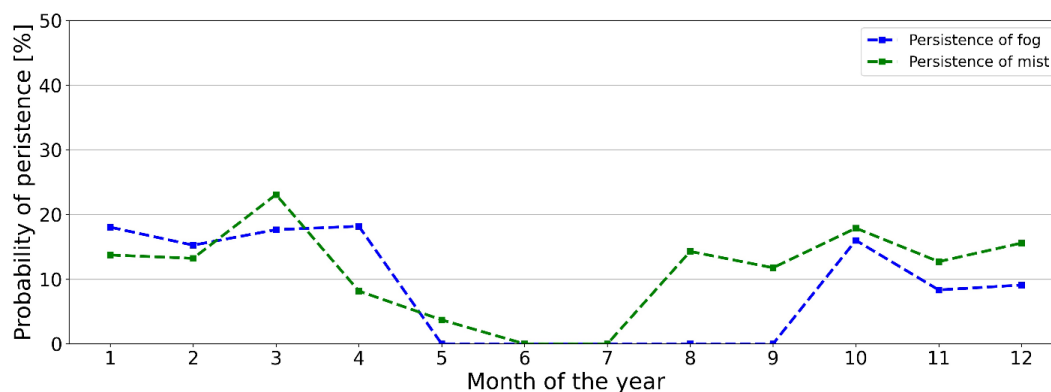


189 **Figure 2. a) Annual number of days with fog (blue line) and mist (green line) at Pula Airport, 2001-2020, with associated**
190 **linear trends and trend equations. b) Average monthly number of days with fog and mist at Pula Airport, the average sea**
191 **temperature measured at the oceanographic station in Pula Bay and the average air temperature measured at the Pula**
192 **Airport, 2021-2020.**
193

194 To obtain a complete picture of fog occurrence over Pula Airport, a climatological analysis was first performed on a
195 large scale and then on a smaller scale. Figure 2a shows the yearly number of days with fog and mist during the period
196 from 2001 to 2020. A day with fog is defined as any day with at least one METAR report indicating observed visibility
197 of less than 1 km and fog being reported at the airport. Similarly, a day with mist is defined as any day with at least
198 one METAR report indicating observed visibility of at least 1 km but less than 5 km (this is the aeronautical definition
199 of mist) and mist being reported at the airport. By adding the condition of fog or mist being reported, situations where
200 reduced visibility was due to precipitation—such as drizzle or rain—were excluded. On average, there are 13.4 days
201 of fog and 45.6 days of mist per year; however, this number is steadily decreasing, as indicated by the pronounced
202 negative trend. The Mann-Kendall statistical significance test shows that this result is statistically significant at the



203 95% confidence level. A careful evaluation of the linear trend reveals that the average number of fog days has
204 decreased by more than 10 days (from 18.4 in 2001 to 8.3 in 2020), and the average number of mist days has decreased
205 by more than 22 days (from 56.8 in 2001 to 34.4 in 2020). A more detailed analysis of fog and mist occurrence, this
206 time in relation to different seasons (Figure 2b), shows that the vast majority of fog and mist (more than 90%) at Pula
207 Airport occurs between October and March. During the observed multi-year period, January is the month with the
208 highest proportion of fog and mist days relative to the total number of days (23% and 20% respectively), followed by
209 February with 21% and 13% respectively, while December stands out only for mist with 17%. In March, October, and
210 November, the share of fog and mist days in the total number of days is 12-13%. Fog at Pula Airport can occur during
211 April and May, but from June to September, fog is an extremely rare phenomenon— for example, in June, there was
212 no recorded fog during the analyzed period from 2001 to 2020. Summarizing the data shows that during the
213 climatological summer (June-July-August), fog occurrence can be expected approximately every six years. The yearly
214 frequency of mist follows a similar pattern, with the only notable difference being that mist is a more frequent
215 phenomenon. The frequency of fog persistence, which is defined as fog occurrence on two consecutive days, is shown
216 in Figure 3. As expected based on previous findings about fog characteristics, persistence can be expected only in the
217 colder part of the year (October-April). From May to September, there have been no recorded instances of fog
218 occurring on two consecutive days. Stable anticyclonic conditions in the cold part of the year are most conducive to
219 fog persistence.



220

221 **Figure 3. Yearly distribution of the climatological probability of persistence (fog occurrence on two consecutive days) of fog**
222 **and mist at Pula Airport, 2001-2020. The probability of persistence is defined as the number of days with persistence relative**
223 **to the total number of days with fog in a given month. Cases where a single fog event was present around midnight (and**
224 **thus spanned two days) were not counted as persistence.**

225 Wind is one of the most important meteorological variables affecting the formation and maintenance of a fog layer,
226 as turbulence generated from wind shear greatly influences the height of the stable boundary layer. Therefore, it is
227 interesting to examine the statistical characteristics of wind during fog episodes. Figure 4 shows wind distributions
228 (data from METAR reports) for all data and for fog/mist conditions in a wind rose plot. In general, the dominant wind
229 at Pula is the NE bora wind, which can easily reach speeds greater than 10 m s^{-1} . Other common winds include
230 westerlies, a consequence of the superimposition of Etesian winds with the sea breeze circulation (Pandžić and Likso,
231 2005; Klaić et al., 2009), as well as north-northeasterly and southeasterly winds. Northwesterly and southwesterly

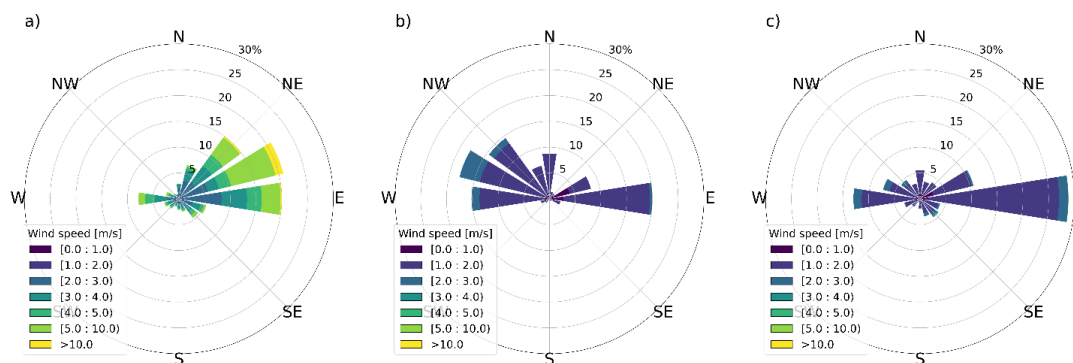


232 winds occur rarely at Pula Airport. The wind rose for fog conditions (Figure 4b) is markedly different; in these
233 situations, W/NW winds are the most common (47.7% of measurements). These winds blow from the direction of the
234 open sea, whereas easterly winds blow from Kvarner Bay, which is dotted with islands and where the sea is deeper.
235 Fog is also commonly encountered when there are light winds from the east, and there were some cases recorded with
236 winds from the north. Southerly winds are almost never associated with fog at Pula Airport. In the majority of cases
237 where fog formed in conditions with easterly winds, wind speed was lower than 3 m s^{-1} . During fog in westerly
238 conditions, wind speeds greater than 3 m s^{-1} are far more common. When mist is reported (Figure 4c), the results are
239 reversed: mist is much more common in situations with easterly winds (28.8% of measurements), which are generally
240 the most frequently observed wind direction at Pula. This is unsurprising since mist is a more frequent phenomenon
241 than fog (Figure 2).

242

243 A closer look at the relationship between wind and visibility/cloud base in fog conditions (Figure 5a-d) provides
244 further evidence of the scarcity of fog in situations with northerly winds. The scatter plot of visibility and wind speed
245 confirms the existence of the aforementioned optimal window of wind speeds—the majority of fog forms when wind
246 speeds are between 0 and 2 m s^{-1} . The same is also observed for low clouds (lower than 200 m) — the majority of low
247 cloud bases were observed at wind speeds of 1 m s^{-1} or less, some between 1 and 2 m s^{-1} , and very few at higher wind
248 speeds. The absence of cloud bases above 300 m at wind speeds higher than 2 m s^{-1} is interesting. Higher wind speeds
249 indicate stronger advection, and personal communication from forecasters confirms that in these cases cloud bases
250 can be very low. This is particularly evident in situations with westerly flows, where fog is more often observed than
251 in easterly flows and where wind speeds are higher. The data for mist conditions (Figure 5e-h) leads to similar
252 conclusions for visibility—mist most often forms in westerly or easterly winds with somewhat higher wind speeds
253 than fog. Mist conditions with cloud bases above 500 m can occur but are rare, and one noteworthy difference between
254 mist and fog is the higher number of mist events with a low cloud base in southeasterly and southwesterly winds.

255



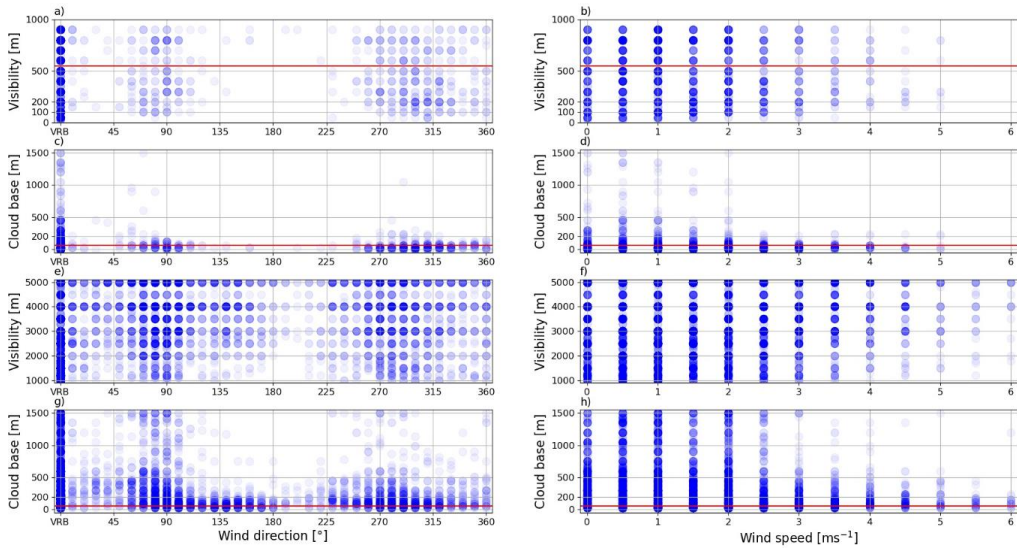
256

257

258

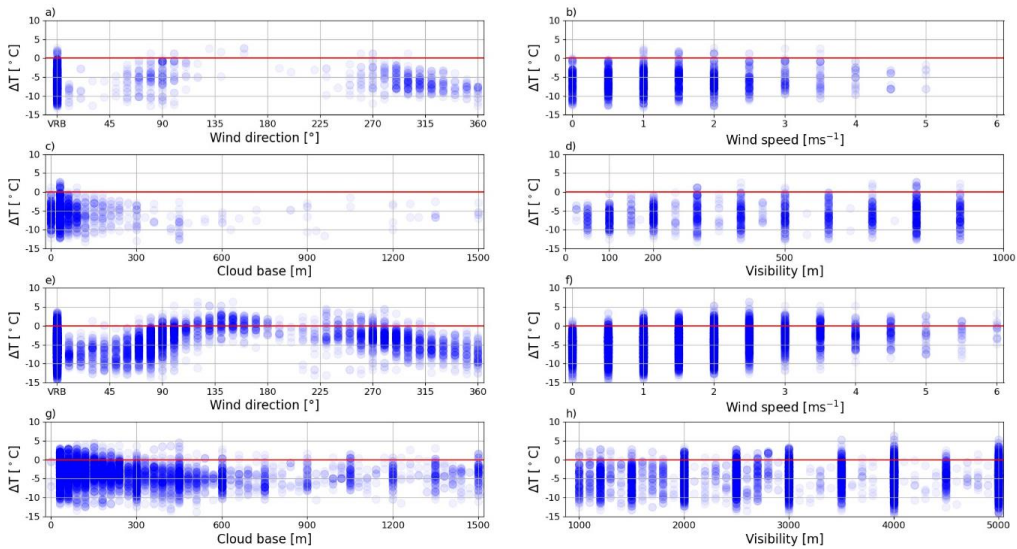
259

Figure 4. Wind rose plots for Pula Airport, for dataset in the period 2001-2020: (a) the whole dataset, (b) fog conditions (c) mist conditions. Data includes only reports where the variation in direction is less than 60° according to ICAO definition. These account for 74 % of total data, 36 % of data in fog conditions and 39% of data in mist conditions.



260
 261 **Figure 5.** Scatter plots of various meteorological parameters for fog conditions (a-d) and mist conditions (e-h) at Pula
 262 Airport, 2001-2020. Circles are colored according to the frequency of data points (darker – more frequent). Red lines mark
 263 the limits for Category I takeoff-landing procedures mentioned in Chapter 2.

264
 265



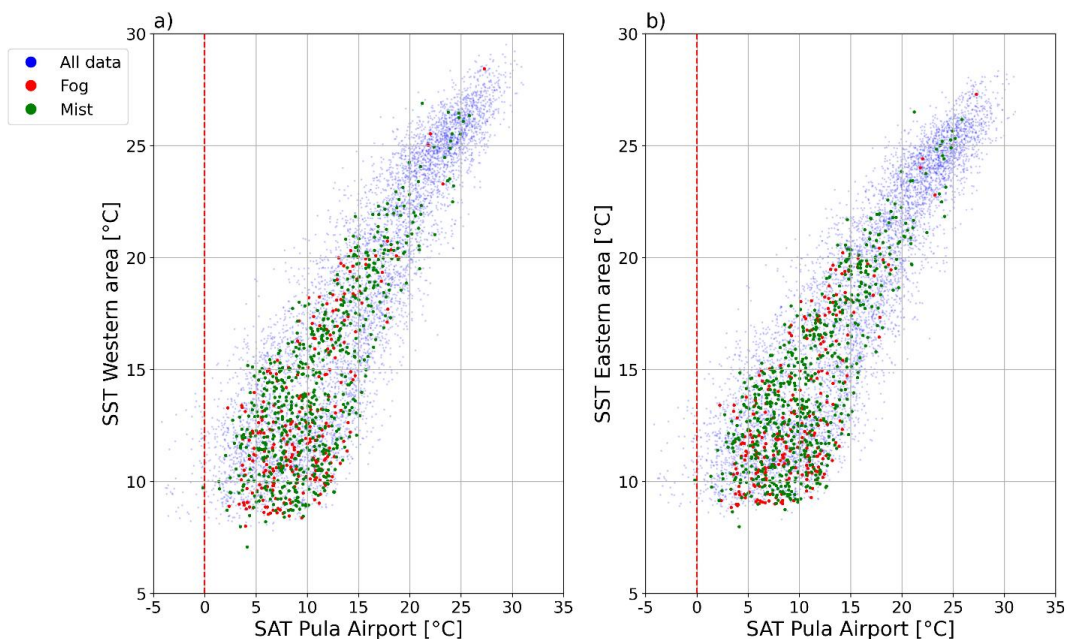
266
 267 **Figure 6.** Scatter plots of air-sea temperature difference between Pula Airport and Pula oceanographic station and various
 268 meteorological parameters at fog initiation (a-d) and mist initiation (e-h), 2001-2020. Circles are colored according to the
 269 frequency of data points (darker – more frequent). Red lines mark the 0 °C difference between air and sea temperature.

270
 271



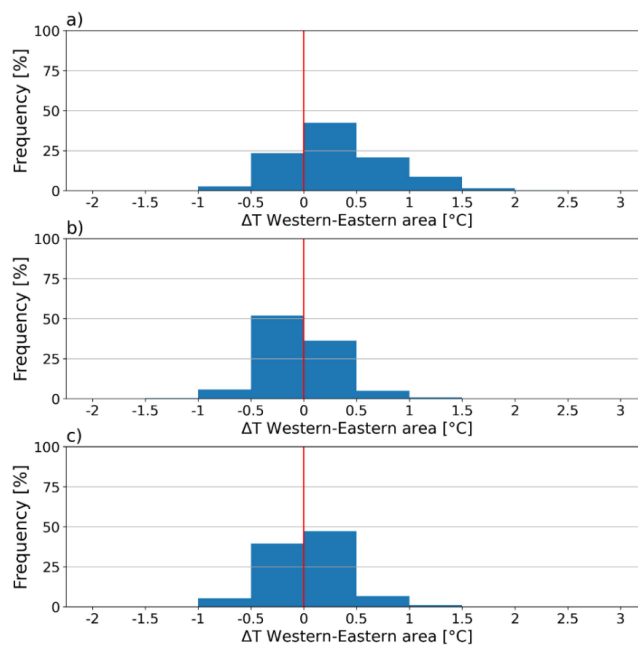
272 Another way to examine fog occurrence is by analyzing the meteorological conditions prior to/at the time of fog
273 formation, as has been done in some previous studies (Tardif and Rasmussen, 2007; Veljović et al., 2015; Zoldoš and
274 Jurković, 2016), or by investigating the difference between air and sea surface temperature for marine fog (Li et al.,
275 2022). Since this study investigates fog at a coastal location, it would be of interest to investigate the difference
276 between air temperature (SAT) and SST (SAT-SST) during fog. For this purpose, SAT data from METAR reports at
277 Pula Airport were compared with SST data from the oceanographic station in Pula Bay, in the immediate vicinity of
278 the city of Pula. Figures 6a-d show scatterplots of the SAT-SST difference and various parameters at fog initiation
279 (first METAR report with visibility <1000 m), and the same is shown in Figure 6e-h for mist initiation. In general, the
280 majority of fog and mist cases form when there is a negative SAT-SST difference, i.e., when SST is higher than the
281 air temperature. Fog is a rare phenomenon during southerly winds (wind direction 135-225°), but mist in these
282 conditions is more common, especially in southeasterly winds (Figure 6e). During SE, S, and SW winds with mist
283 conditions, the SAT-SST difference is close to zero. In 97.4% of fog data, the SAT-SST difference was less than 0,
284 and in only 2.6% of data was it greater than or equal to zero. In mist conditions, there are slightly more cases where
285 the SAT-SST difference was greater than or equal to 0 (7.4%), but still the balance heavily favors warm sea-cold land
286 conditions.

287
288 Although the influence of SST was estimated by comparing the SAT values of the airport and the SST values of the
289 oceanographic station, a more comprehensive picture emerges when the influence of the sea to the west and east of
290 the airport is assessed. For this purpose, the satellite SST values were used for the area west and east of the airport
291 (Figure 1b), over which the two most prevailing winds at Pula Airport are common during fog formation. The SAT
292 and SST values were plotted in two scatter plots for the eastern and western areas for all observations, for observations
293 with fog, and observations with mist (Figure 7). A visual inspection shows that fog and mist usually occur when the
294 SAT-SST pairs have lower values. However, a closer look reveals that the data for fog (red dots) are more widely
295 distributed on the graph for the western region, indicating a greater scattering of observations for SST. This is
296 confirmed by calculations, which show that variance for SST of the western area (for observations with fog) is 12.62
297 °C, and for the eastern area, it is 11.37 °C. The same is true for observations with mist (16.24 and 14.66 °C,
298 respectively). Further insight into the influence of SST on fog formation was gained by separately analyzing the
299 differences between the SST of the western and eastern areas in cases with and without fog or mist (Figure 8). The
300 area west of Pula is generally warmer when neither fog nor mist is present, but fog occurs more frequently when the
301 SST of the eastern area is higher, while the opposite is true for mist. These results can be related to the wind rose
302 statistics for fog and mist (Figure 4), which shows that during fog, the prevailing wind is W-NW (promoting SST
303 decrease in the western area), while during mist, the prevailing wind is E (promoting SST decrease in the eastern area).
304 The temperature differences rarely exceed 0.5°C.



305

306 **Figure 7.** Scatter plots of satellite sea surface temperature (SST) for western area (a) and eastern area (b), and surface air
307 temperature (SAT) at Pula Airport, 2001.-2020.



308

309 **Figure 8.** Histograms of satellite SST difference between the western and eastern area for observations without fog or mist
310 (a), fog (b) and mist(c).



311 3.2 GNG analysis of synoptic weather patterns

312 In this analysis, the GNG method was applied to extract characteristic temporal and spatial patterns of wind and MSLP
313 fields that favor the formation of fog and mist in the Pula region. The GNG analysis was performed on a monthly
314 basis for the entire period analyzed; i.e., all January data, February data, etc., were entered separately in order to
315 calculate them. The reason for this approach is that it makes the results easier to interpret, captures seasonality, and
316 reduces the computational load, which is important given the large hourly dataset involved. To save computational
317 resources, the GNG algorithm was applied only to 10-m wind data from ERA5, and the derived pressure fields were
318 subsequently extrapolated. To obtain an appropriate synoptic situation with large wind systems, such as anticyclones
319 and cyclones affecting the northern Adriatic, a large area in the Mediterranean was selected for analysis (Figure 1b).
320 The 40-year period of ERA5 data (from 1979 to 2019) provided long time series data from which the GNG analysis
321 could learn, enabling the derivation of more accurate and robust spatio-temporal patterns. The one-year discrepancy
322 in the overlap of the ERA5 and fog datasets, particularly in 2020, is a consequence of the fact that the GNG analysis
323 was performed prior to the start of this paper and the computational resources required for a new analysis were no
324 longer available. Given that wind was the primary variable and MSLP the derived variable, wind exerted the
325 predominant influence, thus excluding the occurrence of very strong cyclonic (MSLP < 1000 hPa) or anticyclonic
326 (MSLP > 1030 hPa) formations in the results. However, from a conceptual point of view, and with regard to the
327 dynamic interaction between high- and low-pressure systems, the results are satisfactory and align well with the
328 climatology of the region. To facilitate the observation of broader wind patterns, only wind fields over the sea were
329 visualized. This choice was made because wind patterns over the sea are more uniform and consistent than wind
330 patterns over land, where local variations such as topography or land features can have a large influence on the results.

331
332 This process resulted in 9 Best Matching Units (BMUs) for each month (a total of 108 BMUs) distributed over hourly
333 data, representing the weather patterns with the highest data variance. The hourly data were aggregated into daily data
334 by identifying the most frequent BMU within a day. Subsequently, each day with fog/mist in the 2001-2019 period
335 was associated with the dominant BMU for that day, resulting in a synoptic weather pattern classification for fog/mist
336 days at Pula Airport. To focus on the prevailing synoptic patterns that contribute to the formation of fog and mist,
337 months with more than 10% of days with fog and mist were arbitrarily selected (Table 1). These months are in the
338 colder part of the year and together account for more than 85% of the foggy days of the year. A criterion relating to
339 BMUs was also arbitrarily defined for each month: Only BMUs with more than 15% representation in a given month
340 were selected (Table 1) and plotted (Figures 9-14). In this way, 2 to 4 BMUs were selected and more closely analyzed
341 for each month.

342

343

344

345

346



347 **Table 1. Display of the most frequent Best Matching Units (BMUs) (whose monthly share is greater than 15 percent)**
 348 **describing the prevailing synoptic weather pattern during the days with fog and mist for the selected month at Pula Airport,**
 349 **2001-2019. Blue colored denotes BMU common (>15 % share) for fog and mist, green colored for fog only and red colored**
 350 **for mist only. The slope coefficients describe the linear trends of the most common BMUs, i.e. the yearly change in**
 351 **frequency.**

Month	BMU	Synoptic pattern	Wind	Slope coeff.	Frequency (fog)		Frequency (mist)	
					#	%	#	%
January	BMU-1-6	Quasi-non-gradient-field	WNW, W	-0.390	30	54 %	68	39 %
	BMU-1-8	Cyclone over northern Adriatic (MSLP<1008 hPa)	WNW, NW	0.107	11	20 %	39	23 %
February	BMU-2-5	Anticyclone over central/western Europe (MSLP>1028 hPa)	NE, NNE	0.006	8	16 %	13	12 %
	BMU-2-6	Quasi-non-gradient-field	W, SW	-0.138	17	33 %	36	32 %
March	BMU-3-1	Anticyclone over southeastern Europe (MSLP>1022 hPa)	S, SE	-0.572	16	16 %	5	16 %
	BMU-3-3	Cyclone over northern Adriatic (MSLP<1006 hPa)	SE	-0.051	6	19 %	25	25 %
	BMU-3-8	Quasi-non-gradient-field	S, SE	0.255	11	35 %	31	39 %
October	BMU-10-1	Anticyclone over southeastern Europe (MSLP>1018 hPa)	NE	0.158	4	16 %	13	11 %
	BMU-10-5	Anticyclone over southeastern Europe (MSLP>1020 hPa)	SE	-0.272	10	40 %	38	32 %
	BMU-10-6	Quasi-non-gradient-field	W	-0.051	4	16 %	27	23 %
November	BMU-11-5	Anticyclone over eastern Europe (MSLP>1024 hPa)	SE	0.251	8	24 %	23	21 %
	BMU-11-7	Quasi-non-gradient-field (MSLP>1022 hPa)	WSW, W	-0.415	6	18 %	29	26 %
	BMU-11-9	Anticyclone over southeastern Europe (MSLP>1026hPa)	NE	-0.041	11	33 %	28	25 %
December	BMU-12-1	Anticyclone over southeastern Europe (MSLP>1026 hPa)	NE	-0.000	7	21 %	31	21 %
	BMU-12-3	Cyclone over southern Adriatic (MSLP<1008 hPa)	NE	0.266	5	15 %	23	15 %
	BMU-12-4	Cyclone over the Tyrhennian Sea (MSLP<1008 hPa)	NE	-0.470	6	18 %	14	9 %
	BMU-12-8	Anticyclone over central and eastern Europe (MSLP >1030 hPa)	NE	-0.130	3	9 %	23	15 %

352

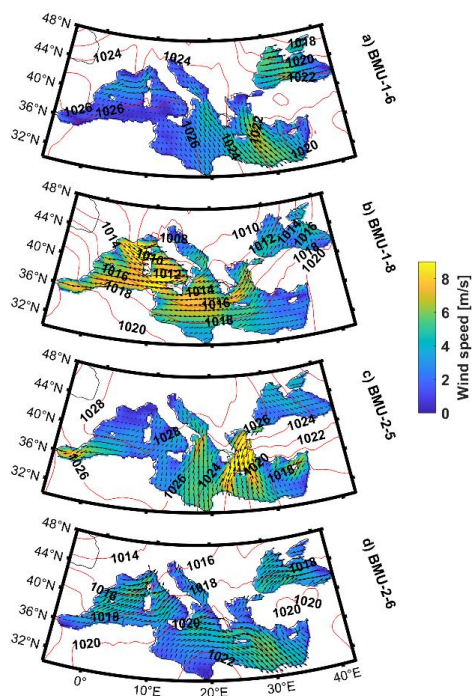
353 The analysis of synoptic patterns favoring fog formation (Table 1) shows that in January, the prevailing synoptic
 354 conditions favoring fog and mist in Pula are characterized by the dominance of a quasi-non-gradient field over the
 355 entire region (BMU-1-6, Figure 9a), where the mean pressure gradient is very weak (Belušić Vozila et al., 2021). This
 356 stable atmospheric pattern supports the maintenance of a relatively calm and stagnant air mass over Pula, which
 357 inhibits the dispersion of pollutants and moisture, promoting fog formation in the area. The second most common
 358 synoptic pattern that favors the formation of fog and mist is the one with a cyclone over the northern Adriatic (BMU-
 359 1-8, Figure 9b). Both synoptic patterns support weak WNW/NW winds over the Istrian peninsula. A similar synoptic
 360 pattern can be observed during the transition to the months of February and March. Again, the quasi-non-gradient
 361 field is the most common pattern suitable for the formation of fog and mist in February (BMU-2-6, Figure 9d) and



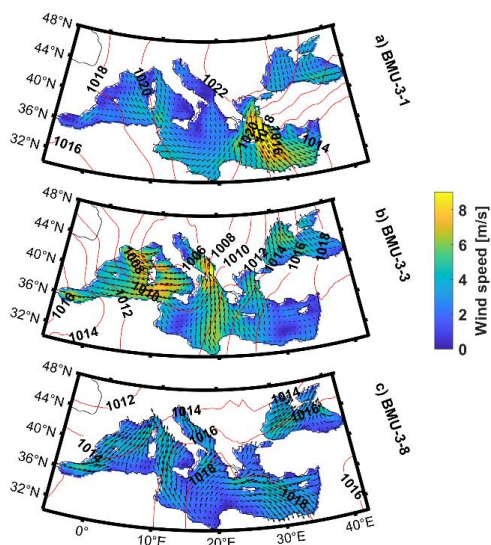
362 March (BMU-3-8, Figure 10c), but compared to January, weak W and SW winds are also present in February, and
363 weak S and SE winds are present in March. In addition to the quasi-non-gradient field, the favorable synoptic patterns
364 in February and March also include anticyclones in the continental part of Europe (BMU-2-5, Figure 9c and BMU-3-
365 1, Figure 10a) and cyclones in the northern Adriatic (BMU-3-3, Figure 10b). Few fog events occur in Pula from April
366 to September, so the BMU results cannot reveal any clear patterns. The limited occurrence of fog during this period
367 is attributed to the lower relative humidity and more stable atmospheric conditions typical for summer in this area.
368 Nevertheless, local factors such as the sea/land breeze and coastal geography may play a role in the occurrence of fog.
369 Consequently, any analysis based on these months should be treated with caution, as the number of recorded fog
370 events is low.

371

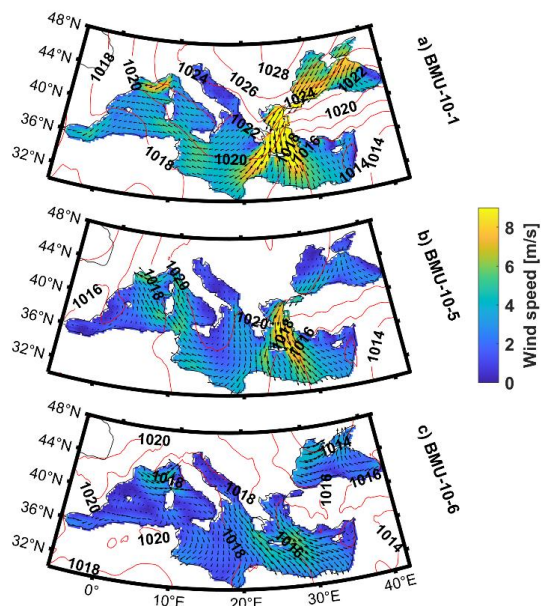
372 At the beginning of October, the synoptic conditions that favor the occurrence of fog and mist in Pula are typically
373 characterized by an area of high pressure over continental Europe, with the most common position being where the
374 center of the high-pressure area is over southeastern Europe, supporting SE winds (BMU-10-5, Figure 11b). This
375 anticyclonic trigger persists into November, accompanied by a strengthened mean pressure field and intensified
376 synoptic pressure gradients over the central Mediterranean. These conditions favor the development of fog in the
377 region (BMU-11-9, Figure 12c). The intensified synoptic pressure gradients over the central Mediterranean contribute
378 to increased NE wind patterns. This increased wind activity can result in moist air being transported from the sea to
379 the coastal regions, providing an additional source of moisture for fog formation. The convergence of air masses along
380 these enhanced pressure gradients can also promote upward movements, leading to local cooling and increased
381 humidity. Pula's coastal location further reinforces the influence of the anticyclone. Coastal areas are more susceptible
382 to temperature inversions due to their proximity to the sea, which retains heat and reduces temperature fluctuations.
383 Anticyclonic conditions over Eastern Europe combined with coastal geography create an environment where cool,
384 moist air is trapped near the surface, favoring the formation of fog. The conditions that favor mist formation are
385 somewhat varied; the most common synoptic pattern is the one where the high-pressure area is located over the
386 western Mediterranean and WSW winds blow over the Istrian peninsula. In addition to the anticyclone, a quasi-non-
387 gradient field with weak W winds also occurs in October and November (BMU-10-6, Figure 11c and BMU-11-7,
388 Figure 12b). In December, the prevailing synoptic weather pattern associated with fog and mist becomes more difficult
389 to recognize – the frequency of the most common BMUs is more evenly distributed, and in addition, more dynamic
390 synoptic conditions prevail (similar to February and March). Nevertheless, the most frequent synoptic pattern for fog
391 and mist (BMU-12-1, Figure 13a and BMU-12-8, Figure 13d) has anticyclonic dominant features. Under these
392 conditions, the Pula region is under the influence of a pressure ridge, with the prevailing weak wind patterns from the
393 northeast further increasing the probability of fog formation. Compared to the previous months, there is also a
394 pronounced influence of cyclones on the formation of fog and mist in December, in two respects: on the one hand, by
395 a weak SE wind due to a cyclone in the southern Adriatic (BMU-12-3, Figure 13b) and on the other hand by a stronger
396 NE wind due to a strong cyclone in the Tyrrhenian Sea (BMU-12-4, Figure 13d).



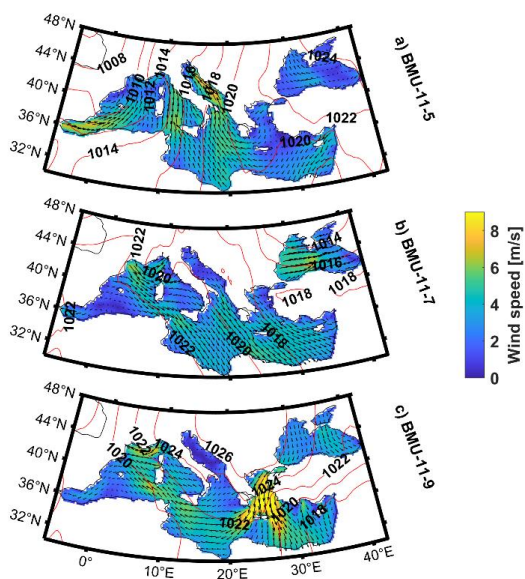
397
398 **Figure 9.** Most prevailing best Matching Units (BMUs) describing synoptic patterns favoring the formation of fog and
399 mist at Pula airport in January (a-b), February (c-d).



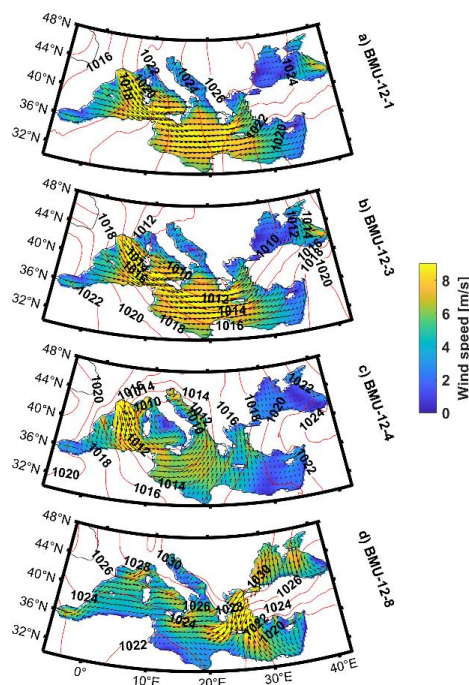
400
401 **Figure 10.** Most prevailing best Matching Units (BMUs) describing synoptic patterns favoring the formation of fog and
402 mist at Pula airport in March (a-c).



403
404 **Figure 11.** Most prevailing best Matching Units (BMUs) describing synoptic patterns favoring the formation of fog and
405 mist at Pula airport in October (a-c).



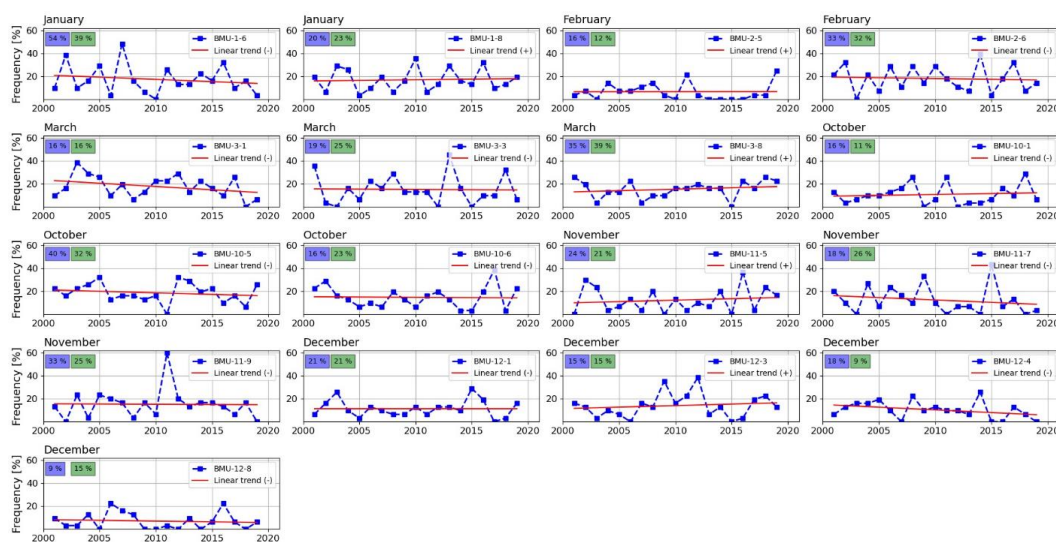
406
407 **Figure 12.** Most prevailing best Matching Units (BMUs) describing synoptic patterns favoring the formation of fog and
408 mist at Pula airport in November (a-c).



409
410
411
412

Figure 13. Most prevailing best Matching Units (BMUs) describing synoptic patterns favoring the formation of fog and mist at Pula airport in December (a-d).

413 In addition to observing the prevailing synoptic patterns during the occurrence of fog and mist, the GNG analysis also
414 enables the investigation of the time series of frequencies of individual BMUs. This was done by first calculating the
415 relative monthly frequency of each BMU for each year, and then using linear regression to estimate a trend and
416 calculate slope coefficients. This ultimately offers insight into changes in the frequency of each BMU throughout two
417 decades (Table 1, Figure 14). In January, it can be seen that the more common BMU-1-6 shows a strong negative
418 trend, while the less frequent BMU-1-8 shows a weaker positive trend. In February, the most common BMU (BMU-
419 2-6) shows a weak negative trend. In March, the most common BMU (BMU-3-8) shows a positive trend, while the
420 frequency of BMU-3-1 shows a strong negative trend. In October, there is a decrease in the most common BMU for
421 fog and mist (BMU-10-5), while November and December show major changes in the frequency of less common
422 BMUs. Analyzing the data by counting the positive and negative changes and dividing the synoptic patterns into three
423 groups (cyclonic/anticyclonic/quasi-non-gradient field) shows that of the 17 BMUs, 8 are anticyclonic, 5 are quasi-
424 non-gradient field, and 4 are cyclonic. There is no trend for 1 BMU (BMU-12-1) in the anticyclonic patterns; 3 BMUs
425 increase in frequency and 4 BMUs decrease in frequency over the years. For quasi-non-gradient, there is 1 increase
426 and 4 decreases. Of the 4 cyclonic BMUs, 2 increase in frequency and 2 decrease. In addition, a strong decrease (slope
427 coefficient >0.3 or <-0.3) is observed in BMU-3-1 (anticyclonic), BMU-1-6 (quasi-non-gradient field), and BMU-12-
428 4 (cyclonic). Positive trends do not have such large values for the gradient coefficient.



429
 430 **Figure 14. Relative frequencies and trends of most common (monthly share in days with fog/mist greater than 15%) BMUs**
 431 **for fog and mist in Pula Airport, data period: 2001-2019. Numbers shaded in blue denote the share of a BMU for fog days,**
 432 **numbers shaded in green denote the share of a BMU for mist days.**

433 **4 Discussion and conclusion**

434 This comprehensive climatological analysis of fog and mist occurrences at Pula Airport from 2001 to 2020 has
 435 provided valuable insights into the changing patterns of these meteorological phenomena. Given that the occurrence
 436 of fog in the eastern Adriatic has been rarely studied, with the last studies conducted 50 years ago (Stipančić, 1972),
 437 there was a strong need for new insights. In summary, instead of the prevailing purely statistical approach to fog and
 438 mist occurrence, a dual approach was chosen that combines classical statistics with neural networks, integrating
 439 measured airport data with synoptic parameters that favor fog and mist formation. This was particularly important, as
 440 the airport's meteorologists already had operational experience regarding which weather patterns, in conjunction with
 441 SST, favor fog formation, but this knowledge had not yet been scientifically published.

442
 443 One of the first important results is the statistically significant decreasing trend in the frequency of fog and mist in the
 444 region, consistent with similar observations in Europe, such as at Zagreb Airport (Zoldoš and Jurković, 2016) or
 445 Milano Airport (Mariani, 2009). While the decreasing trend in Zagreb and Milan can be largely attributed to a
 446 reduction in air pollutants, this conclusion is more difficult to draw for Pula, as it is a much smaller city with less
 447 developed industry, whose impact on the neighboring suburban/rural areas is not as great. The decrease in fog and
 448 mist frequency has been observed in Europe, but the effect is most pronounced in continental Europe and not so much
 449 in the Mediterranean region (Vautard et al., 2009). Apart from the common negative trend, the annual distribution of
 450 fog at Pula Airport, where 90% of events occur from October to March, is also comparable to the annual distribution
 451 of fog events at Zagreb Airport (Zoldoš and Jurković, 2016).

452



453 The second important climatological finding is that, in recent decades, the maximum occurrence of fog in the winter
454 months has shifted from February to January. While February used to be the foggiest month at Pula Airport, with an
455 average of 3.5 foggy days (Stipaničić, 1972), the most recent data show that January has become the foggiest month
456 with 3.05 foggy days (Figure 2b). February remains the second foggiest month, with an average of 2.95 foggy days.
457 This result underscores the importance and value of long data series, which can provide crucial information such as
458 this shift in fog frequency.

459

460 The third climatological conclusion is that fog is most likely to occur with westerly and northwesterly winds (47.7%
461 of measurements), while mist is most common with weak easterly winds. Additionally, compared to continental
462 locations such as Zagreb Airport (Zoldoš and Jurković, 2016), more fog occurs at Pula Airport at wind speeds
463 exceeding 3 m s^{-1} . Conversely, fog at moderate or strong winds ($> 3 \text{ m s}^{-1}$) is less common at Pula Airport than in
464 locations bordering the open ocean, such as the coast of California, where fog often forms at wind speeds above 10 m
465 s^{-1} (Filonczuk et al., 1995). Another finding is that fog rarely forms in calm or very low wind conditions, suggesting
466 that there may be an optimal window of wind speeds that favor fog formation; this part remains open for future
467 investigation. Gultepe et al. (2007) emphasized the importance of wind speed and its influence on turbulence and heat
468 fluxes at the surface, which in turn significantly affect fog occurrence. It is important to note that these results are only
469 based on data where the wind direction is not variable (VRB), i.e., where the change in direction is less than 60° , as
470 defined by the ICAO (International Civil Aviation Organization). The total proportion of non-VRB data is 74%
471 overall, 36% for fog conditions, and 39% for mist conditions.

472

473 As a second approach to gaining insights into fog and mist events at Pula Airport, the Growing Neural Gas (GNG)
474 method was used to analyze the synoptic patterns (BMUs) that favor fog formation at Pula Airport. Fog and mist
475 occurrences are most pronounced in the colder part of the year, but the GNG allowed for a deeper analysis. The
476 majority of the fog events in the cold season occur during stable anticyclonic or quasi-non-gradient field conditions
477 (13 in total), although some events also occur during low-pressure conditions (4 in total). In January, February, and
478 March, anticyclonic and quasi-non-gradient fields were the most frequent patterns, while the cyclone field was the
479 second most frequent in January and March. In October and November, anticyclonic and quasi-non-gradient fields
480 predominated uniformly, contrasting with December, where anticyclonic and cyclonic patterns coincided. These
481 machine learning results are consistent with the empirical knowledge of airport forecasters (personal communication),
482 who concluded that two weather types are most frequently associated with fog in Pula. The first is a predominantly
483 westerly flow bringing in moist air from the west (W) and northwest (NW) during anticyclonic conditions. The second
484 weather type is a predominantly easterly flow with advection from the southeast (SE) during a weakening anticyclone.
485 January and February are precisely the months in which the most frequent pattern is a quasi-non-gradient field
486 characterized by weak westerly winds in the Istrian area, and March is the month in which the SE wind dominates in
487 more than 60% of cases. An interesting exception is December, which deviates from this rule and is dominated by NE
488 winds. Combining the two approaches by comparing the GNG results with the wind rose, it can be seen that the
489 dominance of W/NW winds (more than 60% of cases) significantly contributes to January being the month with the



490 most fog and mist days (Figure 4, Table 1). Considering the total number of fog and mist days in January, it is not
491 surprising that this wind type can have a large share in the overall annual variability of winds favorable for fog.
492 However, the third approach, which involves the use of satellite SST data, must also be considered. If we take into
493 account W/NW winds, which advect air at low speed over the warm sea west of the coast of Istria, the result is clear:
494 warm, humid air is transported over the cold surface around the airport, supporting the formation of fog and mist.
495 Another conclusion, which again refers to the GNG results, the wind rose, and the SST, points to December. In
496 December, fog is caused by weak northeasterly winds, which can result from both low- and high-pressure fields.
497 However, these winds advect air from the east over the enclosed sea of the Kvarner Gulf, which is still warm. This
498 means that warm air still exists above the warm sea surface, which can be advected to the west. Therefore, in January,
499 when the sea in Kvarner has already cooled down significantly, the fog at the airport can be advected from the warmer
500 open sea, which has not yet cooled down sufficiently. In both cases, the SST for both the western and eastern areas is
501 2 to 6 degrees greater than the SAT at the airport.

502

503 Global warming and climate change are the most apparent explanations for the long-term decrease in fog frequency.
504 There are well-documented trends indicating rising temperatures in Pula and surrounding coastal and interior areas of
505 Istria (Bonacci, 2010; Šimunić et al., 2021), increased sea surface temperatures (SST) across the Mediterranean (Pastor
506 et al., 2018) and specifically in Pula (Bonacci, 2023), and growing ocean stratification worldwide over the past 50
507 years (Li et al., 2020). Climatological model reanalyses for the Adriatic region from 1987 to 2017 show positive SST
508 trends for every month of the year. Summer records the most significant increase, although winter months are also
509 experiencing notable rises (Tojčić, 2023). In terms of air temperature, reanalysis indicates that trends are more
510 pronounced from April to September compared to October to March (Tojčić, 2023; Bonacci et al., 2021). Regarding
511 advection fog and mist, wind trends must also be considered. Positive wind trends have been observed over the sea
512 and along the Adriatic coast, ranging between 0.1 and 0.2 m s⁻¹ per decade (Tojčić, 2023). Although these trends are
513 not large enough to overlap the optimal wind speed window for fog, they can significantly alter fog formation
514 mechanisms. For example, the decrease in temperature difference between the sea surface and air (due to rising SST)
515 reduces the temperature gradient, making it harder for air to cool to the dew point required for fog formation.
516 Additionally, higher SSTs result in increased evaporation rates, which, combined with favorable winds, can lead to
517 fog advection. In addition to local factors such as SST, air temperature and wind, changes in synoptic patterns that
518 favor fog or mist formation can be linked to broader synoptic trends over this part of Europe. A decrease in quasi-non-
519 gradient synoptic situations in January, February, October, and November has been documented in the summer months
520 (Belušić Vozila et al., 2021). One significant negative gradient is observed in the BMU cyclone pattern in December,
521 associated with its northward shift (Reyers et al., 2016; Knippertz et al., 2000) and noted in future climate research
522 for this region (Belušić Vozila et al., 2021). However, examining all BMUs with negative trends reveals a total of 10,
523 compared to 6 positive BMUs, and these negative BMUs show a higher frequency of foggy days per month (Table 1).
524 For example, BMU-1-6 has a frequency of 54% in January, BMU-2-6 is 33% in February, and BMU-12-4 is 18% in
525 December. This suggests that the reduction in favorable synoptic situations for fog and mist leads to a decrease in the
526 number of foggy days throughout the study period, outweighing other factors like positive SST trends. Although the



527 similarity to general synoptic system trends is notable, the focus of this work was not on the most common synoptic
528 patterns overall but rather on those showing the highest number of fog and mist days.

529

530 Overall, these results lay a strong foundation for further research and analysis, enabling a deeper understanding of the
531 various meteorological and oceanographic factors that influence fog and mist occurrence at Pula Airport. This is
532 particularly significant as it represents the first scientific study on fog in the Pula area in 50 years, a period during
533 which climate changes have notably altered the local climate. Future projections suggest these changes will become
534 even more pronounced, including lower wind speeds in coastal areas and more extreme contrasts such as increased
535 droughts and heavy precipitation events (Tojčić, 2024). This study has undertaken the broad task of identifying
536 synoptic patterns conducive to fog and mist formation. Since fog and mist formation is primarily influenced by wind
537 speed and moisture advection, there is potential for atmospheric-oceanographic coupled modeling that incorporates
538 finer local topography and improved parameterization of processes at smaller temporal and spatial scales. Such
539 advancements would contribute to a more comprehensive understanding of local meteorological phenomena and their
540 implications for various applications, including aviation meteorology and environmental monitoring.

541 **Code/data availability**

542 All data and codes used in the analysis are available from the corresponding author on request.

543 **Author contribution**

544 Study conception and design, material collection, data preparation and analysis were performed by Marko Zoldoš and
545 Tomislav Džoić. The manuscript was written by Marko Zoldoš, with contribution from Tomislav Džoić in the
546 “Discussion and Conclusion” section. All authors read and approved the final manuscript.

547 **Competing interests**

548 The authors declare that they have no conflict of interest.

549 **Acknowledgments**

550 Frano Matić was supported in part by the European University of the Seas (SEA-EU) alliance through collaborative
551 efforts and resources. Measurements and observations for Pula Airport were provided by the Croatian Air Navigation
552 Service (Crocontrol Ltd.). SST data for Pula were provided by the Meteorological and Hydrological Service of Croatia
553 (DHMZ). SST data in the Mediterranean region were downloaded from the Copernicus Marine Data Store
554 (<https://data.marine.copernicus.eu/>). 10-m wind and mean sea level pressure (MSLP) data were adopted from the fifth
555 generation of ECMWF's ERA5 reanalysis of global climate and weather. Final proofreading (grammar/spelling check)
556 was performed by ChatGPT from OpenAI.



557 References

- 558 Allan, S.S., Gaddy, S.G., Evans, J.E.: Delay causality and reduction at the New York City airports using terminal
559 weather information systems, Massachusetts Institute of Technology, Lincoln Laboratory, Project Rep. ATC-291,
560 2001
- 561 Belo-Pereira, M., Santos, J.A.: A persistent wintertime fog episode at Lisbon airport (Portugal): performance of
562 ECMWF and AROME models, *Meteorol. Appl.* 23, 353-370, doi:10.1002/met.1560, 2016
- 563 Bendix, J.: Fog Climatology of the Po Valley, *Riv. Meteorol. Aeronau.*, 54(3-4), 25-36, 1994
- 564 Belušić, A., Prtenjak, M.T., Güttler, I., Ban, N., Leutwyler, D., Schär, C.: Near-surface wind variability over the
565 broader Adriatic region: insights from an ensemble of regional climate models. *Clim. Dyn.* 50, 4455-4480,
566 doi:10.1007/s00382-017-3885-5, 2018
- 567 Belušić Vozila, A., Telišman Prtenjak, M., Güttler, I.: A Weather-Type Classification and Its Application to Near-
568 Surface Wind Climate Change Projections over the Adriatic Region. *Atmosphere* 12, 948,
569 doi:10.3390/atmos12080948, 2021
- 570 Bergot, T., Koračin, D.: Observation, Simulation and Predictability of Fog: Review and Perspectives. *Atmosphere*
571 12(2), 235, doi:10.3390/atmos12020235, 2021
- 572 Bonacci, O. (2010): Analysis of mean annual temperature series in Croatia, *Građevinar*, 62(9), 781-791,
573 <https://hrcak.srce.hr/59611>, 2010
- 574 Bonacci, D., Patekar, M., Pola, M.: Increasing Trends in Air and Sea Surface Temperature in the Central Adriatic Sea
575 (Croatia), *Journal of Marine Science and Engineering* 9, 4: 358, doi:10.3390/jmse9040358, 2021
- 576 Bonacci, O.: Relationship between sea surface temperature (SST) and surface air temperature (SAT) along the eastern
577 Adriatic Coast of Croatia, *Vodoprivreda*, 55, 325/326; 167-183, 2023
- 578 Džoić, T., Zorica, B., Matić, F., Šestanović, M., Čikeš Keč, V.: Cataloguing environmental influences on the
579 spatiotemporal variability of Adriatic anchovy early life stages in the eastern Adriatic Sea using an artificial neural
580 network, *Front. Mar. Sci.* 9, 997937, doi:10.3389/fmars.2022.997937, 2022
- 581 Filonczuk, M.K., Cayan, D.R., Riddle, L.G.: Variability of Marine Fog along the California coast, *Scripps Institution*
582 *of Oceanography Report* 95-2, 102 pp., 1995
- 583 Fritzke, B.: A growing neural gas network learns topologies, *Adv. Neural Inf. Process. Syst.*, 7, 625-632, 1995
- 584 Gultepe, I., Milbrandt, J.A.: Microphysical Observations and Mesoscale Model Simulation of a Warm Fog Case
585 during FRAM Project, *Pure Appl. Geophys.* 164, 1161-1178, doi:10.1007/978-3-7643-8419-7_4, 2007
- 586 Gultepe, I., Tardif, R., Michaelides, S.C., Cermak, I., Bott, A., Bendix, J. et al.: Fog research: A review of past
587 achievements and future perspectives, *Pure and Appl. Geophys.*, 164(6-7), 1121-1159, doi:10.1007/s00024-007-0211-
588 x, 2007
- 589 Hersbach, H.; Bell, B.; Berrisford, P.; Hirahara, S.; Horányi, A.; Muñoz-Sabater, J. et al. (2020a): The ERA5 global
590 reanalysis, *Q. J. R. Meteorol. Soc.*, 146, 1999-2049, doi:10.1002/qj.3803, 2020
- 591 Hersbach, H.; Bell, B.; Berrisford, P.; Biavati, G.; Horányi, A.; Muñoz-Sabater, J. et al. (2020b): ERA5 Hourly Data
592 on Pressure Levels from 1979 to Present, Copernicus Climate Change Service (C3S) Climate Data Store (CDS),
593 doi:10.1002/qj.3803, 2020



- 594 Huang, B., Zhang, J., Cao, Y., Gao, X., Ma, S., Sun, C.: Improvements of Sea Fog Forecasting based on CMA-TYM,
595 Front. Earth Sci. 10: 854438, doi: 10.1016/j.jastp.2022.105958, 2022
- 596 Ju, T., Wu, B., Zhang, H., Liu, J.: Parameterization of Radiation Fog-Top Height and Methods Evaluation in Tianjin,
597 Atmosphere 11(5), 480, doi:10.3390/atmos11050480, 2020
- 598 Klaić. M.: Analysis of influence of katabatic flows on formation of fog around Zagreb, M. Sc. thesis, University of
599 Zagreb, Croatia, 2015
- 600 Klaić Z. B., Pasarić Z., Tudor M.: On the interplay between sea-land breezes and etesian winds over the Adriatic, J.
601 Mar. Sys. 78 101–118, doi: 10.1016/j.jmarsys.2009.01.016, 2009
- 602 Knippertz, P., Ulbrich, U., Speth, P.: Changing cyclones and surface wind speeds over the North Atlantic and Europe
603 in a transient GHG experiment, Clim. Res. 2000, 15, 109–122, doi:10.3354/cr015109, 2000
- 604 Koračin, D., and Dorman, C.E. (Eds): Marine Fog: Challenges and Advancements in Observations and Forecasting,
605 Springer Atmospheric Sciences Series, Springer International Publishing, Cham, Switzerland, 537 pp.,
606 doi:10.1007/978-3-319-45229-6_7, ISBN 978-3-319-45227-2, 2017
- 607 Koračin, D., Lewis, J., Thompson, W.T., Dorman, C.E., Businger, J.A.: Transition of stratus into fog along the
608 California coast: Observations and Modeling, J. Atmos. Sci., 58, 1714-1731, doi:10.1175/1520-
609 0469(2001)058%3C1714:TOSIFA%3E2.0.CO;2, 2001
- 610 Kulkarni, R., Jenamani, R.K., Pithani, P., Konwar, M., Nigam, N., Ghude, S.D.: Loss to Aviation Economy Due to
611 Winter Fog in New Delhi during the Winter of 2011-2016, Atmosphere, 10(4), 198, doi:10.3390/atmos10040198,
612 2019
- 613 Li, G., Cheng, L., Zhu, J., Trenberth, K.: Increasing ocean stratification over the past half-century, Nat. Clim. Change
614 10(12):1-8, doi:10.1038/s41558-020-00918-2, 2020
- 615 Mariani, L.: Fog in the Po Valley: Some meteo-climatic aspects, Ital. J. Agrometeorol. 3: 35-44, 2009
- 616 Martinetz, T.M., Schulten, K.J.: A Growing Neural Gas Network Learns Topologies, in: Proceedings of the
617 International Conference on Artificial Neural Networks 1991, 397-402, 1991
- 618 Matic, F., Džoić, T., Kalinić, H., Čatipović, L., Udovičić, D., Juretić, T. et al.: Observation of Abrupt Changes in the
619 Sea Surface Layer of the Adriatic Sea, J. Mar. Sci. Eng., 10, 848, doi:10.3390/jmse10070848, 2022
- 620 Merchant, C. J., Embury, O., Bulgin, C. E., Block, T., Corlett, G. K., Fiedler et al.: Satellite-based time-series of sea-
621 surface temperature since 1981 for climate applications, Sci. data 6(1), 1-18, doi: 10.1038/s41597-019-0236-x, 2019
- 622 Omazić, B., Telišman Prtenjak, M., Prša, I., Belušić Vozila, A., Vučetić, V., Karoglan, M., Karoglan Kontić, J., Prša,
623 Ž., Anić, M., Šimon, S., Güttler, I.: Climate change impacts on viticulture in Croatia; viticultural zoning and future
624 potential, Int. J. Climatol., 40, 5634 – 5655, doi:10.1002/joc.6541, 2020
- 625 Oztaner, Y.B., Yilmaz, A.: An Examination of Fog and PM10 Relationship for Ataturk and Esenboga International
626 Airports of Turkey, in: Proceedings of the 6th Atmospheric Science Symposium - ATMOS 2013, Istanbul Technical
627 University, 2013
- 628 Pandžić K., Likso T.: Eastern Adriatic typical wind field patterns and large-scale atmospheric conditions, Int. J.
629 Climatol. 25, 81–98, doi:10.1002/joc.1085, 2005



- 630 Pastor, F., Valiente, J.A., Palau, J.L.: Sea Surface Temperature in the Mediterranean: Trends and Spatial Patterns,
631 Pure and Appl. Geophys., 175, 4017-4029, doi:10.1007/s00024-017-1739-z, 2018
- 632 Pawłowicz, R.: M_Map: A mapping package for MATLAB, version 1.4m, [Computer software], available online at
633 www.eoas.ubc.ca/~rich/map.html, 2020
- 634 Popović, R., Kulović, M., Stanivuk, T.: Meteorological Safety of Entering Eastern Adriatic Ports, Trans. Marit. Sci.
635 2014, 01: 53-60, doi:10.7225/toms.v03.n01.006, 2014
- 636 Reyers, M., Moemken, J., Pinto, J.G.: Future changes of wind energy potentials over Europe in a large CMIP5 multi-
637 model ensemble, Int. J. Climatol. 2016, 36, 783–796, doi:10.1002/joc.4382, 2016
- 638 Stipaničić, V.: Fog on the western coast of the Istria peninsula, Vijesti Pomorske meteorološke službe, 18, 7-10,
639 https://library.foi.hr/dbook/cas.php?B=1&item=S02101&godina=1972&broj=00001, 1972
- 640 Stolaki, S.N., Kazadzis, S.A., Foris, D.V., Karacostas, Th.S.: Fog characteristics at the airport of Thessaloniki, Greece,
641 Nat. Hazards Earth Syst. Sci., 9: 1541-1549, doi:10.5194/nhess-9-1541-2009, 2009
- 642 Šantić, D., Piwosz, K., Matic, F., Vrdoljak Tomaš, A., Arapov, J., Dean, J. L. et al.: Artificial neural network analysis
643 of microbial diversity in the central and southern Adriatic Sea, Sci. Rep. 11, 1–15, doi:10.1038/s41598-021-90863-7,
644 2021
- 645 Šimunić, I., Likso, T., Husnjak, S., Bubalo Kovačić, M.: Analysis of Climate Elements in Central and Western Istria
646 for the Purpose of Determining Irrigation Requirements of Agricultural Crops, Agric. Conspec. Sci. 86(3):225-233,
647 https://hrcak.srce.hr/file/382381, 2021
- 648 Tardif, R., Rasmussen, R.M.: Event-based climatology and typology of fog in the New York City region, J. App.
649 Meteorol. Climatol., 46: 1141-1168, doi:10.1175/JAM2516.1, 2007
- 650 Telišman Prtenjak, M., Grisogono, B.: Sea-land breeze climatological characteristics along the northern Croatian
651 Adriatic coast, Theor. Appl. Climatol., 90, 201–215, doi:10.1007/s00704-006-0286-9, 2007
- 652 Telišman Prtenjak, M., Klaić, M., Jeričević, A., Cuxart, J.: The interaction of the downslope winds and fog formation
653 over the Zagreb area, Atmos. Res. 214: 213-227, doi: 10.1016/j.atmosres.2018.08.001, 2018
- 654 Telišman Prtenjak, M., Viher, M., Jurković, J.: Sea-land breeze development during a summer bora event along the
655 north-eastern Adriatic coast, Q. J. Roy. Meteorol. Soc., 136, 1554–1571, doi:10.1002/qj.649, 2010
- 656 Tešić, M., Brozinčević, K.: Fog phenomenon on the eastern coast of the Adriatic Sea, Hidrografski godišnjak 1974,
657 91-116, 1974
- 658 Tojčić, I., Denamiel, C., Vilibić, I.: Kilometer-scale trends and variability of the Adriatic present climate (1987–2017),
659 Clim. Dyn. 61, 2521-2545, doi: 10.1007/s00382-023-06700-2, 2023
- 660 Tojčić, I., Denamiel, C., Vilibić, I.: Kilometer-scale trends, variability, and extremes of the Adriatic far-future climate
661 (RCP 8.5, 2070-2100), Front. Mar. sci. 16, 907–926, doi:10.3389/fmars.2024.1329020, 2024
- 662 Tudor, M.: Impact of horizontal diffusion, radiation and cloudiness parametrization schemes on fog forecasting in
663 valleys, Meteorol. Atmos. Phys., 108: 57-70, doi:10.1007/s00703-010-0084-x, 2010
- 664 Vautard, R., Yiou, P., van Oldenborgh, G.: The decline of fog, mist and haze in Europe during the last 30 years, Nat.
665 Geosci. 2, 115–119, doi:10.1038/ngeo414, 2009



- 666 Veljović, K., Vujović, D., Lazić, L.: An analysis of fog events at Belgrade International Airport, *Theor. Appl.*
667 *Climatol.* 119 (1-2), 13-24, doi:10.1007/s00704-014-1090-6, 2015
- 668 WMO, International Meteorological Vocabulary, World Meteorological Organization, Geneva, Switzerland, pp. 141.,
669 1966
- 670 Wang, Y., Niu, S. J., Lv, J. J., Lu, C. S., Xu, X. Q., Wang, Y. Y., et al.: A new method for distinguishing unactivated
671 particles in cloud condensation nuclei measurements: Implications for aerosol indirect effect evaluation, *Geophys.*
672 *Res. Lett.* 46, 14185–14194, doi:10.1029/2019gl085379, 2019
- 673 Zoldoš, M., Jurković, J.: Fog event climatology for Zagreb Airport, *Croatian Met. Journal*, 51(51), 13-26,
674 <https://hrcak.srce.hr/168218>, 2016